

01 Jan 2003

A Continually Online Trained Neurocontroller for the Series Branch Control of the UPFC

Ganesh K. Venayagamoorthy
Missouri University of Science and Technology

Radha P. Kalyani

Follow this and additional works at: https://scholarsmine.mst.edu/ele_comeng_facwork



Part of the [Electrical and Computer Engineering Commons](#)

Recommended Citation

G. K. Venayagamoorthy and R. P. Kalyani, "A Continually Online Trained Neurocontroller for the Series Branch Control of the UPFC," *Proceedings of the International Joint Conference on Neural Networks, 2003*, Institute of Electrical and Electronics Engineers (IEEE), Jan 2003.

The definitive version is available at <https://doi.org/10.1109/IJCNN.2003.1224045>

This Article - Conference proceedings is brought to you for free and open access by Scholars' Mine. It has been accepted for inclusion in Electrical and Computer Engineering Faculty Research & Creative Works by an authorized administrator of Scholars' Mine. This work is protected by U. S. Copyright Law. Unauthorized use including reproduction for redistribution requires the permission of the copyright holder. For more information, please contact scholarsmine@mst.edu.

A Continually Online Trained Neurocontroller for the Series Branch Control of the UPFC

R. P. Kalyani, *Student Member, IEEE*, G. K. Venayagamoorthy, *Senior Member, IEEE*,

Abstract - The crucial factor affecting the modern power systems today is load flow control. The Unified Power Flow Controller (UPFC) provides an effective means for controlling the power flow and improving the transient stability in a power network. The UPFC has fast complex dynamics and its conventional control is based on a linearized model of the power system. This paper presents the design of a neurocontroller that controls the power flow and regulates voltage along a transmission line. The continually online neurocontroller is used for controlling the series inverter of UPFC. Simulation results carried out in the PSCAD/EMTDC environment are presented to show the successful control of UPFC and the power system.

Keywords: Indirect adaptive control, Neuroidentifier, Neurocontroller, Power system, Unified Power Flow Controller (UPFC)

I. INTRODUCTION

With the ever increasing complexities in power systems across the globe and the growing need to provide stable, secure, controlled, economic, and high-quality electric power—especially in today's deregulated environment—it is envisaged that Flexible AC Transmission System (FACTS) controllers are going to play a critical role in power systems [1]. FACTS enhance the stability of the power system both with its fast control characteristics and with its continuous compensating capability. The two main objectives of FACTS technology are to control power flow and increase the transmission capacity over an existing transmission corridor [2].

Gyugyi proposed the Unified Power Flow Controller (UPFC) that is a new generation of FACTS devices in 1991 [3]. It is a device, which can control simultaneously all three parameters of power transmission line (impedance, voltage magnitude and its phase angle). This device combines together the features of two other FACTS devices: the Static Synchronous Compensator (STATCOM) and the Static Synchronous Series Compensator (SSSC). Practically, these two devices are two Voltage Source Inverters (VSIs), one connected in shunt with the transmission line through a shunt transformer and other in series with the transmission line through a series transformer. These VSIs are connected back to back by a common DC link, which is typical a storage capacitor.

Neural networks are suitable for multi variable applications as they can easily identify the interactions between the system's inputs and outputs. Their ability to learn and store information about system nonlinearities allows neural

networks to be used for modeling and designing intelligent controllers for power systems [4, 5]. Thus, offering alternatives for conventional linear and nonlinear control. A radial basis function neural network controller for UPFC based on direct adaptive control has been reported to improve the transient stability performance of a power system [6]. It is known that indirect adaptive control is able to control a nonlinear system with fast changing dynamics, like the power system better, since the dynamics are continually identified by a model.

This paper presents the design of a *neurocontroller* to control the series branch of UPFC in a single machine infinite bus (SMIB) power system setup. The design of the continually online trained (COT) neurocontroller is based on the indirect adaptive control scheme to replace the existing conventional PI controllers in the series branch of a UPFC. It comprises of two neural networks, one called the *neuroidentifier*, to identify the complex nonlinear dynamics of the UPFC and the power system, and the other, for the control. Advantages of neurocontrollers over the conventional controllers are that they are able to adapt to changes in the system operating conditions automatically unlike the conventional controllers whose performances degrade for such changes [4, 5].

II. SINGLE MACHINE INFINITE BUS SYSTEM WITH UPFC

For identifying and controlling the dynamics of a UPFC and the power system, a single machine infinite-bus (SMIB) power system is setup as shown in Fig. 1 in PSCAD/EMTDC environment. This power system comprises of a synchronous generator with exciter-automatic voltage regulator (AVR) and turbine-governor combinations connected to an infinite bus through two sections of transmission lines and the UPFC is placed between the two sections of the transmission lines as shown in Fig. 1. The SMIB with the UPFC is called the *plant* in the rest of the paper. The UPFC functions as an ideal ac-to-ac power inverter in which the real power can freely flow in either direction between the ac terminals of the two inverters, and each inverter can independently generate (or absorb) reactive power at its own ac output terminal.

The series inverter provides the main function of the UPFC by injecting a voltage with magnitude V_2 , which is controllable and a phase angle α in series with the line via an insertion transformer. This injected voltage acts essentially as a synchronous ac voltage source. The transmission line current flows through this voltage source resulting in a reactive and active power exchange between itself

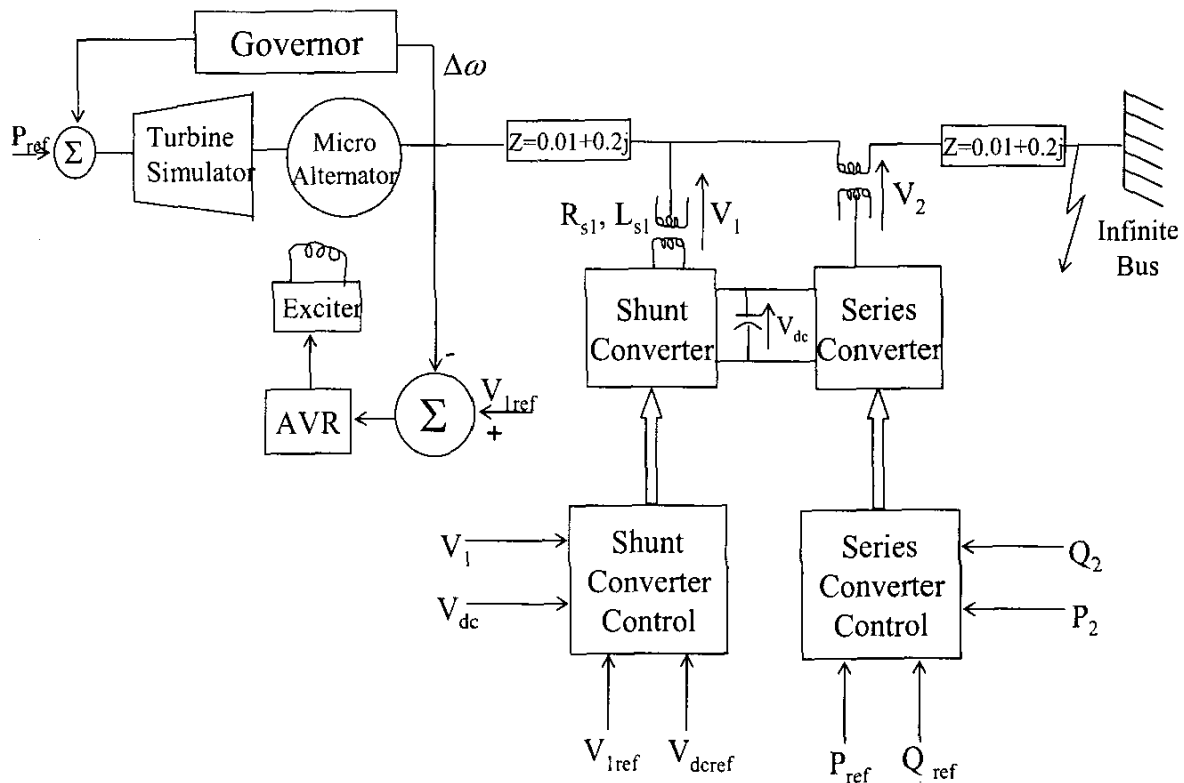


Fig. 1 Single machine infinite bus system with the UPFC (the 'plant').

and the ac system. The inverter generates the reactive power exchanged at the ac terminal internally. The active power exchanged at the ac terminal is converted into dc power, which appears at the DC link as a positive or negative real power.

The basic function of shunt inverter is to generate or absorb the real power demanded by series inverter at the common DC link. The power demand by the series inverter at the DC link is converted back to ac by the shunt inverter and fed to the transmission line bus via a shunt-connected transformer. In addition to this the shunt inverter can also generate or absorb controllable reactive power if desired and thereby provides independent shunt reactive compensation for the line [3].

The three main control parameters of UPFC are voltage magnitude, voltage angle and shunt reactive current. Control of real and reactive power can be achieved by injecting series voltage with an appropriate magnitude and angle. The transient stability model for the shunt and series branch of a UPFC in the dq reference frame are given in [7]. The conventional shunt and series branch control of the UPFC is briefly described below.

A. Shunt Branch Control

Control of the shunt active and reactive current is achieved by varying the shunt inverter voltage active and reactive

components E_{pd} and E_{pq} accordingly. The reactive power flow and shunt input voltage can be regulated by active voltage component E_{pd} and the DC-link capacitor voltage V_{dc} support can be achieved by regulating E_{pq} . Figure 2 shows a block diagram of conventional shunt PI controllers.

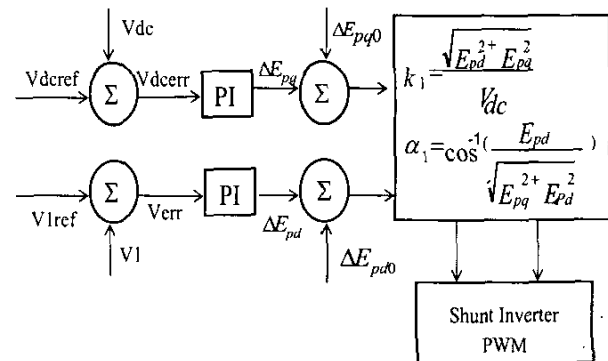


Fig. 2 Shunt branch control of the UPFC.

The outputs of the control system are the modulation index k_1 and phase shift α_1 . The parameters of shunt PI controllers are determined for a given operating condition where the system is linearized, thus the performance of linear controller degrades for changes in the operating conditions. The relevant control equations are given in [7].

B. Series Branch Control

Figure 3 shows the block diagram of the conventional PI controllers for series branch of the UPFC. The control of series converter can be achieved using PQ decoupled control. The outputs of the control system are the modulation index k_2 and phase shift α_2 . Neglecting inverter losses, the injected active and reactive powers as well as output active and reactive powers are given by the equations.

$$P_2 = \frac{V_2(E_q - E_d \cos \delta + E_d \sin \delta)}{X} \quad (1)$$

$$Q_2 = \frac{V_2 E_d \cos \delta + V_2 E_q \sin \delta - V_2 E_d^2 + E_d^2 + E_q^2}{X} \quad (2)$$

$$P_{out} = \frac{V_2^2 \sin \delta + V_2 E_q}{X} \quad (3)$$

$$Q_{out} = \frac{2V_2 E_d \cos \delta + 2V_2 E_q \sin \delta + E_d^2 + E_q^2}{2X} \quad (4)$$

where

$$\begin{aligned} V_2 &= \sqrt{E_d^2 + E_q^2} \\ E_q &= V_2 \sin(\theta_2) \\ E_d &= V_{inj} \cos(\theta_{inj}) \end{aligned}$$

Equation (3) shows that P_{out} is mainly affected by E_q whereas (4) shows that Q_{out} is affected by both E_q and E_d . In incremental form, the line active and reactive power can be expressed in terms of ΔE_q and ΔE_d as given by (6a) and (6b).

$$\Delta P_{out} = \frac{V}{X} \Delta E_q \quad (6a)$$

$$\Delta Q_{out} = \frac{1}{X} (\Delta E_d V \cos \delta + \Delta E_q V \sin \delta + \Delta E_d E_{in} + \Delta E_q E_{qn}) \quad (6b)$$

But we can assume that $\cos \delta$ is close to unity and $\sin \delta$ is close to 0 since the phase angle between two buses on a transmission line is less than 30° , which leads to (7).

$$\Delta Q_{out} = \frac{1}{X} (V \Delta E_d + E_{do} \Delta E_d + E_{qo} \Delta E_q) \quad (7)$$

The conventional PI control for the series branch of UPFC (with the switches S1 and S2 at position 1) is as shown in Fig. 3. The PI controllers are replaced by the neurocontroller with switches S1 and S2 at position 2. The design procedure

of the neurocontroller is explained in section III.

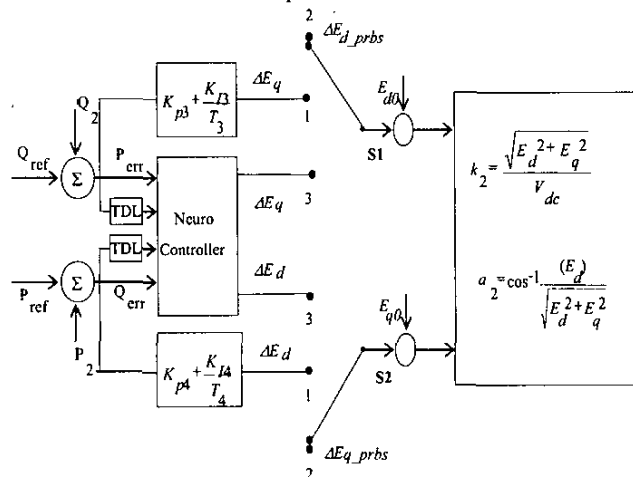


Fig. 3 Series inverter control showing conventional PI controllers, training signals for the neuroidentifier (SENI) and neurocontroller (SENC).

III. DESIGN OF NEUROCONTROLLER

The neurocontroller architecture consists of two separate neural networks, one for the identifier and other for the neurocontroller. The neuroidentifier is used to provide a dynamic model at all times, and the neurocontroller is used to replace the conventional PI controllers (Fig. 3). The training of the neuroidentifier and neurocontroller takes place in two phases, namely a so called *pre-control phase* and a *post-control phase*.

A. Pre-Control Phase

During this training period the neurocontroller and neuroidentifier accept measurements from UPFC but do not control the series branch of UPFC.

1) *Neuroidentifier Pre-control Training:* The identification/modeling of the plant in Fig. 1 is carried out using a neuroidentifier (NI), to identify the series inverter dynamics (Fig. 4). This Series neuroidentifier (SENI) is trained online to dynamically identify the system parameters which are the inputs to PI controller and the neurocontroller at the next time step and which eventually determines the UPFC controller outputs. The neuroidentifier is required for the following reasons: (a) To obtain errors for training the neurocontroller by comparing the output of the desired response predictor [4] to that of the neuroidentifier at time $t+1$ (Fig. 5). (b) To obtain the derivative of these error signals with respect to the neurocontroller's outputs by backpropagating the errors in (a) through the neuroidentifier instead of using calculus of variations (Fig. 5). In the pre-training phase, pseudorandom binary signals (PRBSs) are applied to excite all possible dynamics of the plant [4, 5] and the switches S1 and S2 in Fig. 3 are set to position 2. The SENI is a three layer feed forward neural network with

thirteen inputs, a single hidden layer with fourteen neurons, and two outputs which identifies the dynamics of the plant.

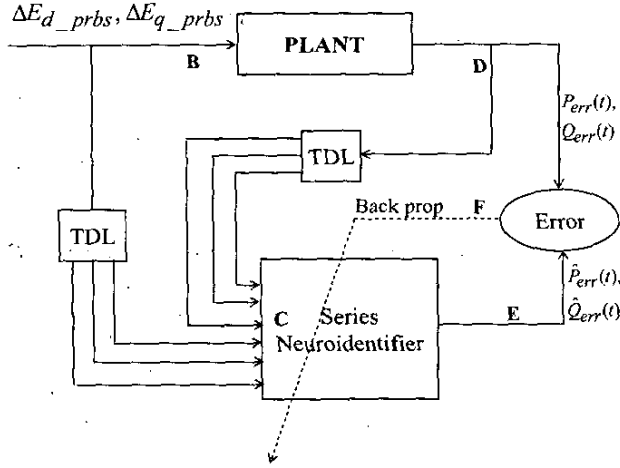


Fig. 4 Pre-control training of SENI for plant identification.

There are four different types of inputs, the first two inputs to the neuroidentifier are the differences between the following signals: the measured real power and its reference value - P_{err} , and, the measured reactive power and its reference value Q_{err} . The other two inputs are the training signals generated using pseudorandom random signals (PRBS) - ΔE_{d_prbs} and ΔE_{q_prbs} . These PRBS signals are only fed to the series inverter and SENI during the pre-training phase with the aid of switches S1 and S2 (Fig. 3). All the four types of inputs are time delayed (TDL) by one sample period and together with their eight previously delayed values form the twelve inputs to the SENI. The outputs of the SENI are estimated difference one time step ahead in the real power - \hat{P}_{err} and the reactive power - \hat{Q}_{err} . The signals at B to the plant and are the PRBS training signals (switches S1 & S2 at position 2). These PRBS signals along with the delayed values of the plant outputs are fed to the SENI at C. The outputs of SENI at E are compared to outputs of the plant at D and error signals at F are used to update the weights of the SENI using the backpropagation algorithm.

2) *Neurocontroller Pre-control Training:* During the pre-training of the SENC, the weights of the SENI are fixed. The SENC is a three layer feed forward neural network with six inputs, a single hidden layer with fourteen neurons and two outputs. Figure 5 depicts the SENC development architecture and, the respective inputs and outputs for the pretraining phase. The PRBS signals are again added to the input of the series branch and SENI as in Fig. 5. The outputs of the plant are fed into the desired response predictor, which predicts $P_{err}(t+1)$ and $Q_{err}(t+1)$ at K. The output of SENI at E is subtracted from the output of the desired response predictor [4] at K to produce the error signal at H which is back propagated through the SENI to obtain $\Delta \hat{u}(t)$. The difference

between $\Delta \hat{u}(t)$ and the outputs of neurocontroller generates the error signal at L which is used to update the weights of the SENC using backpropagation. Pre-training is terminated when the weights of the SENI and SENC have converged over a period of time. The next phase of training (post-control) for the SENI and SENC are carried out while the SENC is allowed to control the plant.

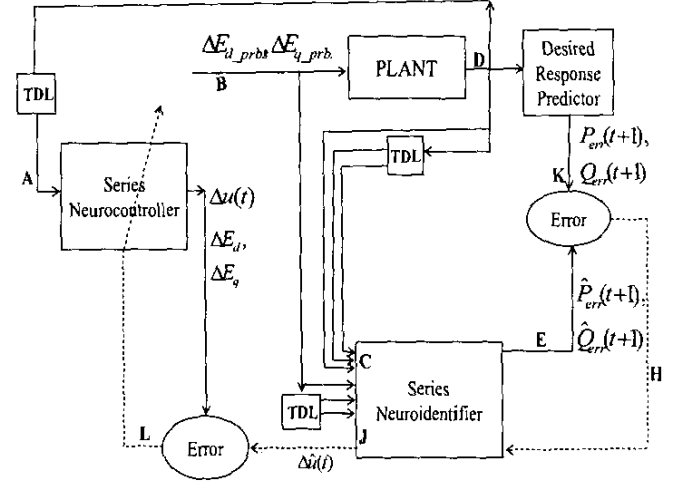


Fig. 5 Pre-control training of SENC.

B. Post- Control Phase:

During this phase, online training of the SENC and SENI continues while SENC is controlling the series branch of the UPFC. The post-control phase training steps for SENI (Fig. 6) and SENC (Fig. 7) are described below. The PRBS signals used in the pre-training phase are now set to zero and outputs for the SENC are substituted.

1) Neuroidentifier Post-control Training (Fig. 6):

1. The plant output signals at D are sampled and time delayed by one, two and three sample periods.
2. The sampled signals from step 1 are input at A to the SENC which then calculates the signals ΔE_d and ΔE_q which are used to train the SENI as well as to control the plant.
3. These control signals are time delayed by one, two and three sample periods, and, together with the signals from step 1 are input to the SENI at C.
4. The outputs at D ($P_{err}(t)$ and $Q_{err}(t)$) and the outputs of SENI at E ($\hat{P}_{err}(t)$ and $\hat{Q}_{err}(t)$) are subtracted to produce error signals at F which are back propagated to update weights of SENI.

2) Neurocontroller Post-control Training (Fig. 7):

5. In the post-control training of SENC, the output of the SENI at E ($\hat{P}_{err}(t+1)$ and $\hat{Q}_{err}(t+1)$), and the desired response at K ($P_{err}(t+1)$ and $Q_{err}(t+1)$) are subtracted to produce a second error signal at H. The error signal at H is back propagated through the SENI and the derivatives

are obtained at **J** with changing the weights of the neuroidentifier fixed.

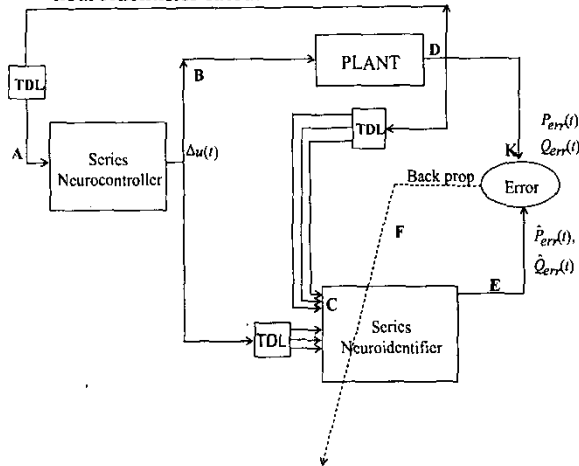


Fig. 6 Post-control training of SENI.

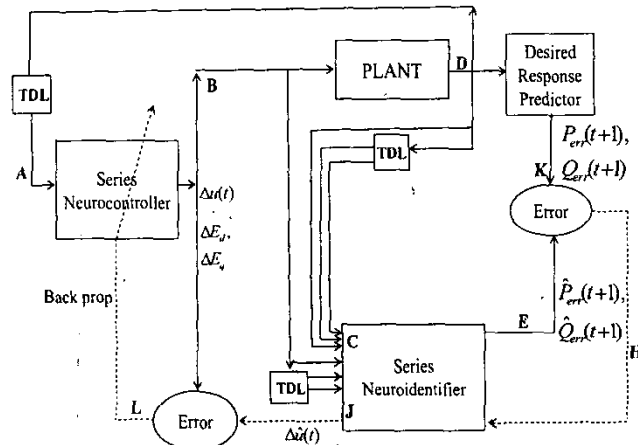


Fig. 7 Post training of SENC.

6. The back propagated signal at **J** is subtracted from the output signal of the SENC to produce an error signal at **L**.
7. This error signal at **L** is then used to update the weights in the SENC, using the back propagation algorithm. This causes the SENC to change its output in a way which drives all the error signals to zero.
8. New control signals are calculated ΔE_d and ΔE_q using the updated weights in step 8 and are then applied at time $(t+1)$ to the plant at **B**.
9. These steps (1 to 10) are repeated for subsequent time periods [4].

IV. SIMULATION RESULTS

The system model comprises of a synchronous generator (590 MVA, 38 KV L-L) [8] operating at real power, $P=0.4$ p.u and reactive power, $Q=0.1$ p.u, with a transmission line impedance of $Z = (0.02 + j0.4)$ p.u. The governor and turbine

models are the IEEE standard models of PSCAD/EMTDC[9]. The parameters of PI controllers are obtained using time response analysis [10]. A sampling frequency of 10 kHz is used to sample the outputs of the plant. The SENI and SENC are trained with a learning rate of 0.06.

The plots below show the terminal voltage and speed of the synchronous generator for three different controllers, namely:

- a) **SENC**: With the UPFC controlled by a *neurocontroller* on the series branch and conventional *PI controllers* on shunt branch.
- b) **PI**: With the UPFC controlled by conventional *PI controllers* on both series and shunt branches.
- c) **No UPFC**: Without a UPFC in the power system.

A 300 ms duration three phase short circuit fault is applied at the infinite bus. Figure 8 shows the terminal voltage response for the three different controllers. Similarly, Fig. 9 shows the corresponding speed signals for the three controllers.

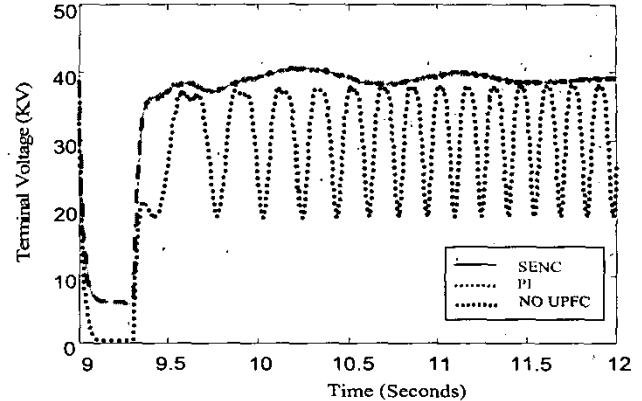


Fig. 8 Terminal voltage response plots for the three different controllers for the synchronous generator operating at $P = 0.4$ p.u and $Q = 0.1$ p.u.

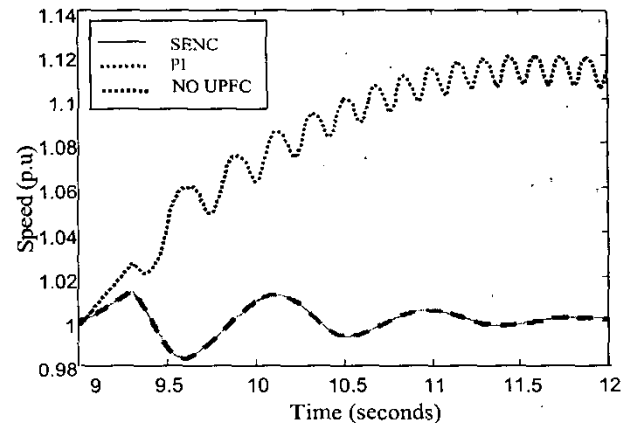


Fig. 9 Speed response plots for the three different controllers for the synchronous generator operating at $P = 0.4$ p.u and $Q = 0.1$ p.u.

No remarkable difference in the SENC is seen from Figs. 8 and 9 since the PI controllers are fine tuned to give their best performance at this operating point ($P=0.4$ p.u and $Q=0.1$ p.u). But it is clearly seen that the UPFC plays an important role in damping the sustained oscillation caused by a large

disturbance (300 ms short circuit). The 300 ms duration is typically unusual but it is chosen in this study to clearly illustrate role of a UPFC. Figures 10 and 11 show the plots of the terminal voltage and speed waveforms for the synchronous generator operating at $P=0.6$ p.u and $Q=0.15$ p.u. It can be seen from the figures that as the operating point changed, a slight difference is noticeable in the SENC and PI performances. This is because of the continual online training carried out on the SENC and not re-tuning the PI controllers' parameters. With the current setup, the shunt branch of UPFC is controlled by conventional PI controllers, thus the full potential of SENC is not exploited and therefore, a dramatic improvement is not noticeable.

The neurocontroller has also been tested at other operating points and observed to provide better damping compared to the PI controllers.

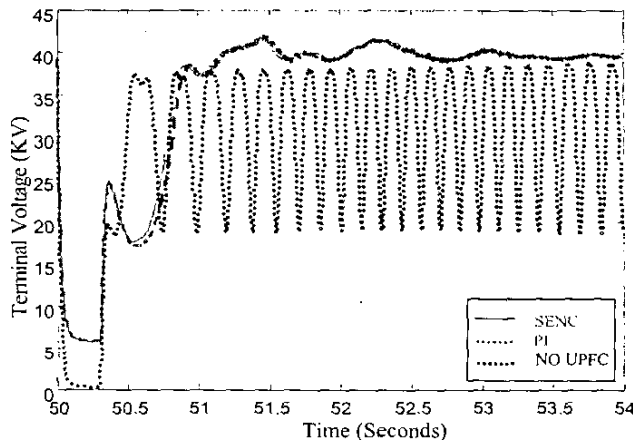


Fig. 10 Terminal voltage response plots for the three different controllers for the synchronous generator operating at $P = 0.6$ p.u and $Q = 0.15$ p.u.

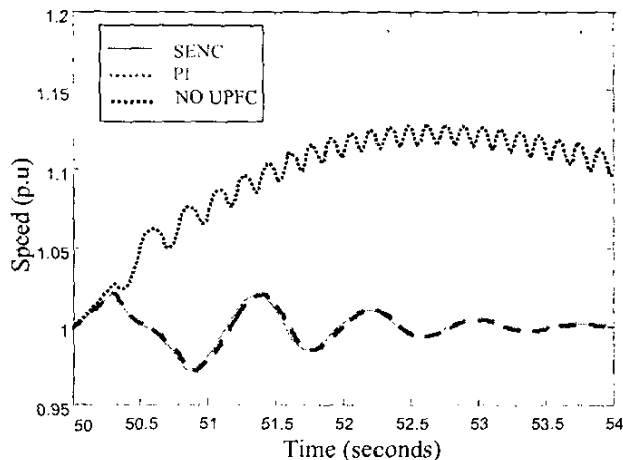


Fig. 11 Speed response plots for the three different controllers for the synchronous generator operating at $P = 0.6$ p.u and $Q = 0.15$ p.u.

V. CONCLUSION

In this paper, the design of a continually online trained neurocontroller to provide adaptive nonlinear control for the series branch of UPFC over a wide range of operating conditions is proposed. It has shown by this work that it is possible for a neural network to identify the complex dynamics of a unified power flow controller and in addition, the power system in which it is connected and another neural network to control the UPFC in *adaptive nonlinear* fashion. A superior performance of the neurocontroller is expected as a result of the online training of neuroidentifier and the neurocontroller which *never* stops. The conventional PI controllers controlling the UPFC shunt branch restricts the full potential of the online trained series neurocontroller designed in this paper. The next step is to design a continually online neurocontroller for the shunt branch of the UPFC. This is currently in progress. Future work involves extending the control strategy to a real power system with multimachines.

ACKNOWLEDGMENT

Financial support from the National Science Foundation (NSF), USA under grant no. ECS-0231632 for this research is gratefully acknowledged.

VI. REFERENCES

- [1] R.M. Mathur, R. K. Varma, *Thyristor-based FACTS controllers for electrical transmission systems*, IEEE Press and John Wiley & Sons, Inc.
- [2] L. Chunlei; S. Hongbo, D.C. Yu, "A novel method of power flow analysis with unified power flow controller (UPFC)" *IEEE Power Engineering Society Winter Meeting*, vol. 4, pp. 2800 -2805.
- [3] N. G. Hingorani, L. Gyugyi, *Understanding FACTS concepts and technology of flexible AC transmission systems*, Power Electronics Sponsored By: IEEE Power Engineering Society.
- [4] G.K. Venayagamoorthy, R.G. Harley, "Two separate continually online-trained neurocontrollers for excitation and turbine control of a turbo generator", *IEEE Transactions on Industry Applications*, vol. 38 no. 3, pp. 887 -893, May/June 2002.
- [5] G.K. Venayagamoorthy and R.G. Harley, "A continually online trained neurocontroller for excitation and turbine control of a turbo generator", *IEEE Trans. on Energy Conversion*, vol.16, no.3, pp. 261-269, September 2001.
- [6] P.K. Dash, S. Mishra, G. Panda, "A radial basis function neural network controller for UPFC", *IEEE Transactions on Power Systems*, vol. 15, no. 4, pp. 1293 - 1299, November 2000.
- [7] M.L. Crow, L.Y. Dong, L. Zhang, "A new control strategy for the unified power flow controller", *IEEE 2002 Power Engineering Society Winter Meeting*, vol. 1, pp. 562 -566.
- [8] Anderson PM, Fouad AA, *Power System Control and Stability*, IEEE Press, New York, 1994, ISBN 0-7803-1029-2.
- [9] Manitoba HVDC Research Centre Inc, *PSCAD/EMTDC manual Version 3.0*, 244 Cree Crescent, Winnipeg, Manitoba, Canada R3J 3W1
- [10] Katsuhiko Ogata, *Modern control engineering (3rd ed.)*, Prentice-Hall, Inc., Upper Saddle River, NJ, 1996